PHYSICAL REVIEW B VOLUME 57, NUMBER 4 15 JANUARY 1998-II

Surface electronic structure of Ge(111) from 300 to 1100 K by metastable deexcitation spectroscopy

L. Pasquali* and S. Nannarone
Istituto Nazionale di Fisica della Materia, Unità di Modena and Department of Physics, University of Modena, Via G. Campi 213/a, 41100 Modena, Italy

M. Canepa and L. Mattera
Istituto Nazionale di Fisica della Materia, Unità di Genova and Department of Physics, University of Genova, Via Dodecaneso 33, 16146 Genova, Italy

(Received 29 April 1997; revised manuscript received 9 September 1997)

Metastable atom deexcitation spectroscopy is applied to the study of the temperature dependence of the electronic structure of the Ge(111)$c(2\times8)$ surface. The present work is stimulated by the debate on temperature induced surface phase transitions. In this field the application of high surface sensitive atomic beam spectroscopy appears to be extremely promising. Metastable deexcitation spectra are taken in the 300–1100 K temperature interval, i.e., up to ~100 K below the bulk melting point. Spectra show a monotonic variation with temperature. Restatom and adatom contributions are identified and their evolution with temperature is followed. In particular, the persistence of the adatoms up to the highest investigated temperatures and the progressive metallization of the surface, already visible since 670 K, are observed. Data seem to indicate more agreement with surface models where order is preserved at high temperatures. [S0163-1829(98)03503-6]

I. INTRODUCTION

Surface phase transitions as a function of temperature have attracted considerable attention in recent years both from theoretical and experimental points of view.[1] A particularly interesting example is represented by the case of Ge(111)$c(2\times8)$. At room temperature the stable surface structure is characterized by adatoms that saturate 3/4 of the ideal dangling bonds and donate their extra electrons to the remaining 1/4 of surface atoms (restatoms). At $T_1 \approx 600$ K the surface undergoes a first (medium-temperature) structure transition leading to a (1×1) low-energy electron diffraction (LEED) pattern.[2] Scanning tunneling microscopy (STM),[3,4] photoemission[5,6] and *ab initio* molecular dynamics calculations[7] have suggested a picture of surface modification in which the $c(2\times8)$ adatom-restatom structure breaks up with the diffusion of the adatoms preferentially along the $\langle 110\rangle$ directions.

A second (high-temperature) structure transition at $T_2 \approx 1050$ K (160 K below the bulk melting temperature $T_m = 1210$ K) was observed by LEED for the first time by McRae and Malic.[8] The model they gave, suggested by the rapid decrease of some diffraction peaks near 1050 K, involved the preservation of the layerlike crystalline order up to the surface and a loss of the lateral long-range order in the outermost double layer. Models based on surface melting or surface roughening were ruled out. Since the first LEED observations, many experimental and theoretical works were devoted to the study of Ge(111) at high temperatures, giving rise to different and partially conflicting pictures. We recall here some significant examples.

Electronic property changes were observed by electron-energy-loss spectroscopy (EELS) (Ref. 9) and were first interpreted in terms of the formation of an amorphouslike layer at the surface at the transition temperature T_2. Similar conclusions were also reached after ellipsometry experiments.[10] A ''layered liquid'' model was later proposed by Denier van der Gon *et al.*[11] after the results of medium-energy ion scattering (MEIS) suggesting the idea on an incomplete melting transition. Support to this model came also from photoelectron diffraction and holography by Tran *et al.*[12] Recently, in a first-principles molecular-dynamics simulation, this picture was supported by Takeuchi, Selloni, and Tosatti[13] who found the first bilayer to be dynamically disordered and metallic. Confirmations came also from a recent EELS experiment,[14] which was interpreted in terms of an abrupt increase in surface optical conductivity at T_2, and from photoemission and photoabsorption experiments,[15,16] in which a metallic surface layer was detected above T_2 with a thickness of about one bilayer.

Contrary to previous reports, a x-ray diffraction experiment[17] indicated a proliferation of random vacancies above T_2 suggesting a continuous change in surface structure with no disordering phase transition.

Finally evidence for an order-order transition was reported by Meli *et al.*[18] who observed with high-resolution helium atom scattering (HAS) sharp integral-order diffraction structures that changed only in their relative amplitudes above T_2, indicating the persistence of long-range (1×1) order in the first bilayer. The model they suggested was based on a surface that remained highly ordered above T_2 and that could be metallic due to the delocalization of the adatoms.

Atomic beams are known to be particularly powerful tools in the investigation of the geometrical structure and dynamics of surfaces. In fact, because of their low kinetic energy and neutrality, atoms do not penetrate into the lattice and induce extremely low perturbation to the system, permitting the achievement of a high surface sensitivity.

Within this context, it appears as extremely useful to exploit the peculiarities of neutral atomic beams not only in the study of the geometrical structure of surfaces but also in the investigation of the surface electronic structure. This can be obtained by using thermal beams of neutral excited metastable atoms.

Metastable atom deexcitation spectroscopy (MDS) has proven during the years to be extremely powerful in the study of the electronic properties of surfaces and low dimensional systems[19] and more recently in the study of clean semiconductor surfaces.[20] The technique is based on an interatomic Auger type deexcitation involving helium metastable atoms impinging on the surface at thermal velocity and surface localized electronic orbitals. Since the interaction concerns preferentially orbitals of the first atomic layer that are oriented towards vacuum, MDS performs surface valence-band spectroscopy with enhanced surface specificity.

For these reasons, and after our recent results on clean GaAs(110),[20] we decided to apply the technique also to the study of Ge(111) as a function of temperature.

For clean semiconductor surfaces deexcitation occurs in two steps: *resonant ionization* (RI) followed by *Auger neutralization* (AN).[20] In the first step the metastable atom in front of the surface is resonantly ionized with the tunnelling of the excited electron into the solid; in the second step the generated ion is neutralized by interatomic Auger process with the participation of two electrons from the solid valence band. The energy distribution of the emitted electrons can be related to the self-convolution of the surface density of states (SDOS) weighted by the Auger matrix element.[20] Usually two different approaches to data analysis can be followed: the *forward* approach consists in attempting to reproduce the experimental spectrum by simulating the interaction, starting from a calculated surface electronic valence-band structure;[21] the *inverse* approach consists in extracting an *effective* SDOS from the spectrum through a deconvolution operation. In the present case the *inverse* method is adopted.

In the present work, MD spectra taken as a function of temperature, from 300 K up to 1100 K, are presented. A preliminary discussion of raw data will be followed by *effective* SDOS calculations through deconvolution operations. Results will be discussed on the basis of the comparison with angle-resolved ultraviolet photoemission spectroscopy (AR-UPS) data and with the theoretical and experimental results reported in literature.

II. EXPERIMENTAL

The experiments were performed at the Department of Physics of the University of Modena in a ultrahigh-vacuum (UHV) experimental system based on two coupled chambers, one specifically intended for sample preparation and the other for spectroscopy. The preparation chamber is equipped with LEED (four grid OPR-304 Riber), an ion gun (Leybold IQ 10/35), and a double pass cylindrical mirror analyzer with coaxial electron gun (Perkin Elmer 15-255-G) for Auger-electron spectroscopy (AES) and EELS. The spectroscopy chamber is equipped with a hemispherical electron analyzer (VG ADES 400) mounted on a goniometer allowing independent rotations in both horizontal and vertical planes, a He windowless differentially pumped discharge lamp emitting

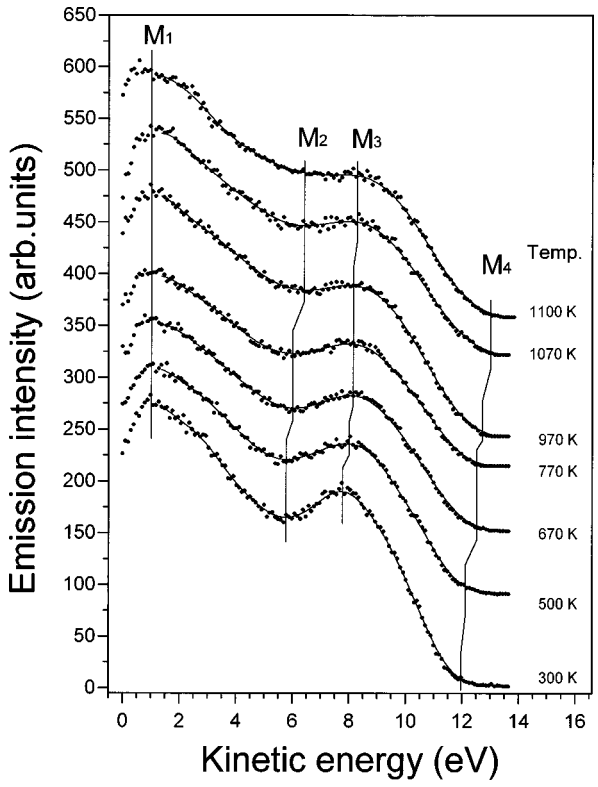

FIG. 1. Metastable deexcitation spectra on Ge(111) from 300 K to 1100 K. The experimental curves are taken under the same experimental conditions. Dots represent experimental spectra, solid line represents FFT filtered spectra.

He I (21.2 eV) and He II (40.8 eV) photons, an electron gun (Leybold EQ 22/35) and a hot cathode supersonic metastable atom source.[22]

During the experiment, the He metastable beam impinged at 45° with respect to the sample normal. The metastable beam intensity was $\sim 10^8$ metastables/s on the sample surface. Electrons were detected and energy analyzed at 45° with respect to the sample normal with a constant resolution of 0.6 eV for MDS. Energy resolution for UPS was 0.4 eV.

The Ge(111) wafer (n-type, Sb doped, 0.1 Ω cm) was mounted on Ta clips and resistively heated. The surface was prepared in situ by cycles of Ar-ion sputtering and annealing up to 1000 K in ultrahigh-vacuum. Surface cleanliness was checked by Auger spectroscopy; surface ordering at room temperature was controlled by LEED. The sample temperature was measured with an infrared pyrometer and with an optical pyrometer, both calibrated with a thermocouple and against the Ge melting point.

In photoemission, E_F position was determined on a gold sample and on the tantalum clips of sample holder.

The base pressure in both chambers was $<1\times10^{-10}$ Torr with the sample at room temperature and never rising above 5×10^{-10} Torr at the highest temperatures reached.

During the measurements the heating current was pulsed at few Hz and data acquisition was suspended during current flowing in the sample.

III. RESULTS

Figure 1 shows the experimental MD spectra taken on

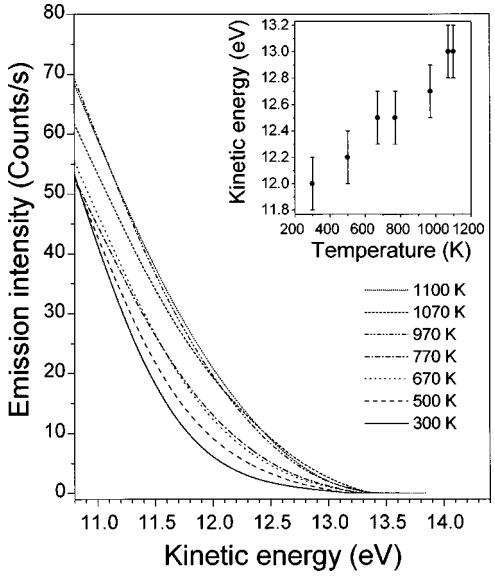

FIG. 2. High-kinetic-energy region magnification of the filtered spectra showing the progressive shift of the onset as the temperature is increased. The inset shows the onset variation as obtained by linear extrapolation on the experimental spectra.

Ge(111) at different temperatures, from 300 K up to 1100 K. Fast Fourier Transform (FFT) smooth filtering was applied to data to reduce high-frequency noise in order to accomplish the deconvolution operations.

All spectra in Fig. 1 present similar shapes and common overall characteristics. Two principal broad features can be identified at about 8 eV and at about 1 eV of kinetic energy, labeled by M_3 and M_1, respectively. A progressive shift of the first structure M_3 maximum towards higher kinetic energies can be noticed with increasing temperatures. A well-defined valley M_2 is present at about 6–7 eV, which is also progressively reduced and shifted towards higher kinetic energies as temperature is increased. Consistently, the high kinetic energy onsets, indicated by M_4 in Fig. 1, as determined by linear extrapolation on the experimental curves,[20] tend to shift towards higher kinetic energies from 12 ± 0.2 eV to 13 ± 0.2 eV for the room-temperature spectrum and for the 1100 K spectrum, respectively. Values obtained for the different temperatures investigated are reported in the inset of Fig. 2 which shows a blow up of the high kinetic energy part of the spectra. The gradual displacement of onsets of the spectra can be observed together with a progressive variation of the curve slope in the high-kinetic-energy region.

Due to the similar excitation energy and sampling region, photoemission is often flanked to MDS as a source of both support and comparison.

Photoemission data are presented in Figs. 3 and 4. Spectra were taken along the $[1\bar{1}0]$ direction with a photon incidence angle of 45° with respect to the sample normal, as indicated in the inset on top of Fig. 3. In Fig. 3 full spectra at three different emission angles and at three example temperatures (300, 770, and 1100 K) are shown.

In Fig. 4 the valence band top is shown at all the temperatures investigated at constant emission angle of 28°.

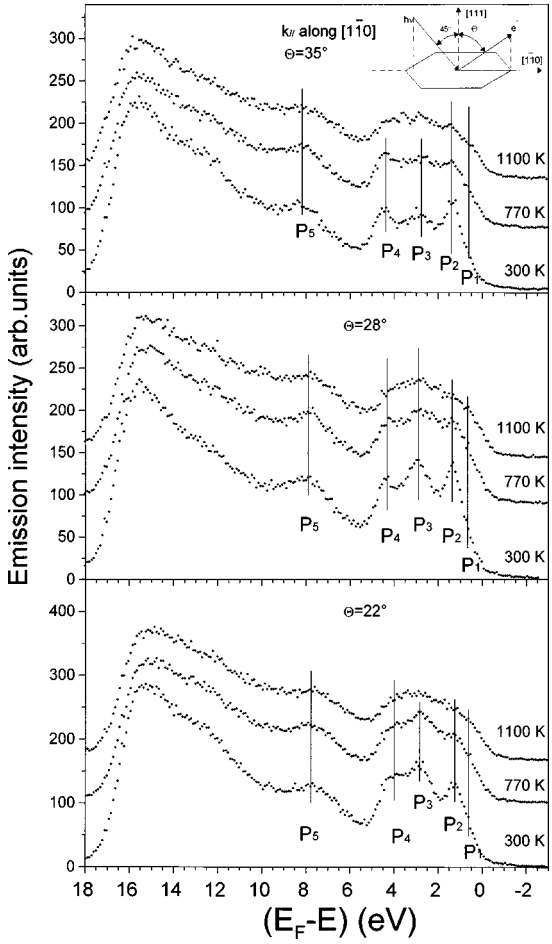

FIG. 3. Photoemission spectra ($h\nu=21.2$ eV) taken at 300, 770, and 1100 K at three different emission angles along the $[1\bar{1}0]$ direction. The experimental geometry is shown in the inset.

IV. DISCUSSION

A. Photoemission results

Starting the discussion of the results from photoemission data, a good correspondence is present between our data at room temperature and other angle-resolved UP spectra reported in literature.[23–26] It can be noticed in Fig. 4 that the spectra show a progressive reduction with temperature of the peak at about 1.4 eV of binding energy and an increasing emission in correspondence of E_F. The same behavior is also observed on the spectra of Fig. 3 and is consistent with previous reported results.[15,16]

The prominent features labeled P_3, P_4, and P_5 in Fig. 3 are related to bulk bands altered by the surface.[23,24,26] The features P_1 and P_2 are surface related structures associated to the adatom-restatom complex. Various authors[23–26] agree in associating the peak P_2 centered at about 1.4 eV of binding energy to the adatom $p_{x,y}$ bonds on the surface. The faint feature labeled by P_1 at about 0.7 eV is associated to the p_z restatom dangling bond.[23–26]

Focussing the discussion on surface state related features, in Fig. 4 at 500 K, before the first structure transition from (2×8) to (1×1), the spectral intensity is still very low at E_F and the P_2 peak is only weakly reduced. After the transition, in the temperature range 670–770 K, this feature, although

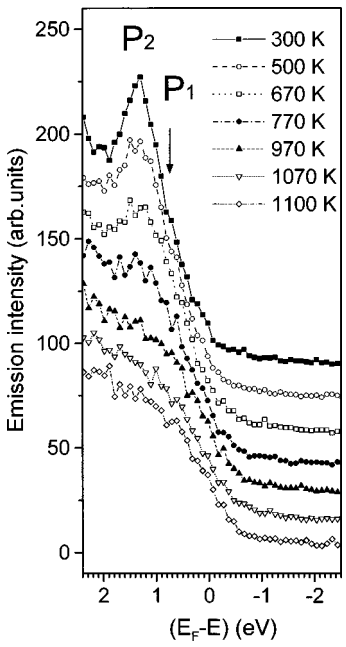

FIG. 4. Photoemission spectra ($h\nu=21.2$ eV) taken at all the investigated temperatures at an emission angle of 28° along the $[1\bar{1}0]$ direction. Only the top of the valence band is shown. Spectra were taken under the same experimental conditions.

reducing, is still present, indicating that the adatom-restatom structure is persistent. Coincidently a definite emission at E_F shows up. This observation is in agreement with scanning-tunneling microscopy (STM) measurements[3,4] and theoretical results,[7] which show the surface demonstrating a structure modification occurring preferentially through an anisotropic adatom diffusion. During the hopping diffusion of the adatoms, electron charge transfer takes place between the initial restatom to the final restatom producing a concentration of surface free carriers as well as a progressive closing of the surface-state gap.

At higher temperatures, the P_2 feature smears out showing an overall agreement with previous data by Goldoni *et al.*[16]

The total estimated shift of the UPS top of the valence band from room temperature to 1100 K is about 0.4 eV, as obtained from Fig. 4, and has to be associated with the variation of the photoelectric threshold ϕ. The low kinetic energy cutoff position of the spectra at increasing temperature was also measured by linear extrapolation of the low-kinetic-energy tail of the secondaries peak. No significant work-function variation was observed within the experimental incertitude.

B. Deconvolution of MD spectra

Focussing now on the MDS results of Fig. 1, let's consider first the spectrum at room temperature and follow the same procedure adopted for GaAs(110) in Ref. 20.

The onset value (12 eV) and the shape of the experimental spectrum are typical indicators of the RI + AN deexcitation process. This is expected for Ge, which presents at room temperature a value of $\phi=4.66$ eV.[27] Similar considerations allow us to conclude that emission is due to RI + AN at all the investigated temperatures.

The maximum kinetic energy of the emitted electrons referred to the vacuum level is given for the RI+AN process by[20]

$$E_{k,\max}=E_{i_{\rm eff}}-2\phi \tag{1}$$

where $E_{i_{\rm eff}}$ is the effective ionization energy of the He $1s$ atomic electron in front of the surface. $E_{i_{\rm eff}}$ takes into account the image charge potential interaction and is given by[19]

$$E_{i_{\rm eff}}=E_i-\frac{(\epsilon-1)3.6}{(\epsilon+1)z_0}\,, \tag{2}$$

where E_i is the atom ionization energy, ϵ the semiconductor dielectric constant ($\epsilon=16$ for Ge (Ref. 27)) and z_0 the most probable distance at which the deexcitation takes place. At room temperature, an estimation of the high-kinetic-energy onset with $E_i=24.6$ eV (for He) and with $z_0=1$ Å gives a value for $E_{k,\max}$ of 12.1 eV, which is in agreement with the experimental value, within the experimental uncertainty.

Moreover, an overall agreement can be found between the present spectrum and previous ion neutralization spectroscopy (INS) results obtained by Sakurai and Hagstrum[28] on Ge(111)$c(2\times8)$ using He ions of 10 eV. Incidently, it is well known[19] that using neutral metastable atoms instead of ions as probes strongly reduces broadening effects on spectra. This permits us to reduce the uncertainty in determining the maximum electron kinetic energy, which is particularly important in data processing and, as in the present case, in detecting small relative variations in different spectra.

Because RI+AN is the deexcitation mechanism, the *effective* SDOS is obtained by performing a deconvolution operation. The spectra have been filtered, in order to reduce the high-frequency noise, and deconvoluted according to the method outlined in Ref. 20 where the surface *effective* SDOS of GaAs(110) was determined. The first derivatives of the spectra were also calculated as a reliability test to the deconvolution procedure. Deconvolutions and derivatives are shown in Figs. 5, 6, and 7. The correspondence of features between deconvolutions and first derivatives of spectra indicates that the unfolding procedure applied is free from numerical artifacts.[20,29]

Deconvolution and the first derivative of the room-temperature spectrum are shown in Fig. 5. The deconvolution curve is reported in binding energy where the zero is referred to the spectrum onset (12 eV of kinetic energy) indicated in the inset of Fig. 2. For ease of discussion, four main regions have been identified, according to the different portions of the SDOS, and have been indicated with labels from I to IV.

According to the present and previous[23–26] photoemission results and theoretical results,[30] the intense feature in region II with maximum at 1.5 ± 0.2 eV of binding energy can be ascribed to surface states of the adatom-restatom complex, where the adatom and the restatom contribute to the high and low binding-energy side of the feature, respectively. The two contributions have been labeled A and R in Fig. 5. The considerable intensity of the structure is in agreement with the charge distribution associated with these surface states that are characterized by orbitals protruding out into the vacuum.

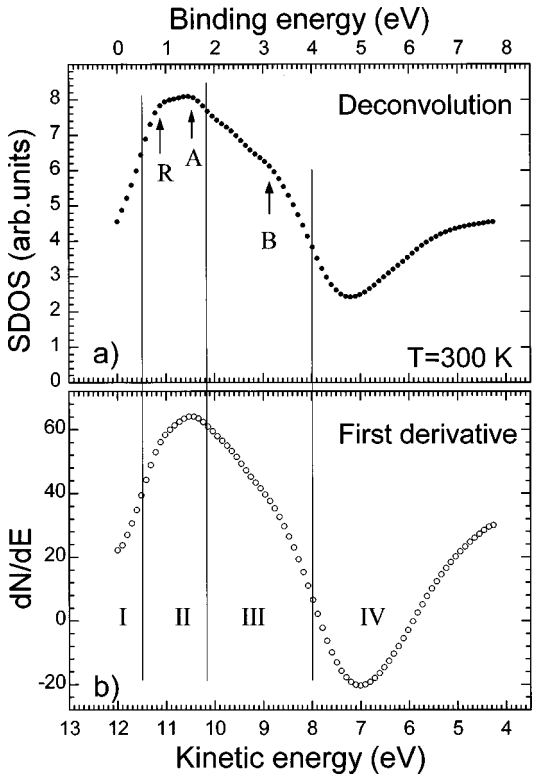

FIG. 5. (a) Deconvolution of the MD room temperature spectrum representing the *effective* SDOS. Deconvolution has been calculated on 80 experimental points following the method outlined in Ref. 20. Four main regions have been identified according to the assignment of the features in the text. (b) First derivative of the filtered experimental spectrum. The correspondence of structures between deconvolution and first derivative is indication of the reliability of the unfolding procedure.

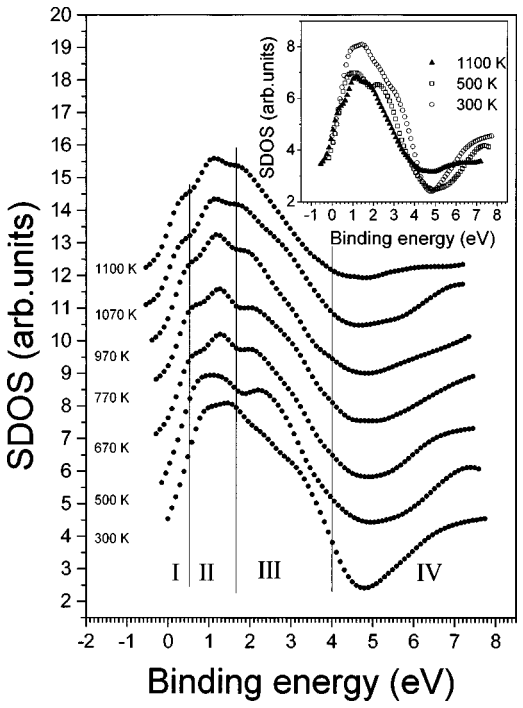

FIG. 6. *Effective* SDOS at different temperatures. Curves are reported in binding energy referred to the room-temperature *effective* SDOS. The four main regions identified in Fig. 5 are also indicated. Inset shows the intensity variations of the features at three temperatures (300, 500, and 1100 K).

The situation is analogous to the case of GaAs(110) where the major spectral contribution was given by the p_z-like surface arsenic atom dangling bond. It is interesting to note that the intensity balance between the adatom and the restatom contributions is altered with respect to UPS. The higher sensitivity of MDS to the restatom comes directly from the p_z nature of the orbital involved.

The shoulder in region III, labeled by *B*, can be associated with surface-modified bulk states that have a lower interaction probability with the metastable atom. Again, the information is different from that obtained by photoemission, which shows well-defined intensity maxima in the same energy region. The position of the intensity minimum in region IV at about 4.8 eV is in good agreement with the corresponding intensity minimum in photoemission measurements and with the intensity minimum of DOS in theoretical calculations.[13,31] It can be associated with the minimum of the bulk DOS.

As far as temperature is concerned, each deconvolution was first calculated separately by taking as origin of each curve the experimental high-kinetic-energy onsets as reported in the inset of Fig. 2. Deconvolutions are reported in Fig. 6 on a binding-energy scale, where the zero of binding energy refers to the origin of the room-temperature curve. By assuming a negligible variation of $E_{i_{\text{eff}}}$ [Eq. (1)] with temperature and by using Eq. (1) together with the values of the high-kinetic-energy onsets shown in the inset of Fig. 2, the other curves are shifted horizontally with respect to the one at room temperature, in order to take into account the photoelectric edge change. This way of displaying the curves emphasizes the variation of the *effective* SDOS with temperature with respect to the room-temperature case. Consequently, the contributions of *effective* SDOS at negative binding energy indicate the occurrence of states closer to the

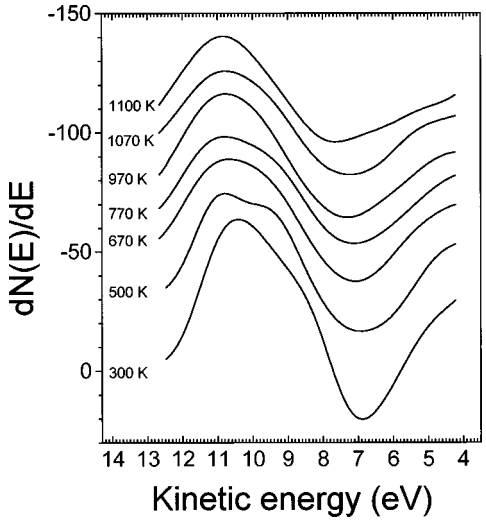

FIG. 7. First derivatives of filtered experimental spectra as an internal test for the reliability of the deconvolution procedure. The good correspondence between first derivative and deconvolution features is an index that mathematical artifacts are not introduced during the unfolding operation.

vacuum level. Similarly, features showing up at the same binding energies are fixed with respect to the vacuum level.

In principle, onset changes can be due to work-function variations together with, according to Eq. (1), modifications of $E_{i_{\mathrm{eff}}}$ and ϕ. Work-function variations can be ruled out as specified above when discussing photoemission results. Concerning ϕ, however, by assuming $E_{i_{\mathrm{eff}}}$ constant with temperature and by using the data of Fig. 2 and Eq. (1), it can be estimated that ϕ undergoes a monotonic reduction with temperature giving a value of 0.5 ± 0.2 eV for its overall change between room temperature and 1100 K. This value is in close agreement with the estimation of 0.4 ± 0.2 eV obtained by photoemission. This gives support to the assumption of the temperature independence of $E_{i_{\mathrm{eff}}}$. In this respect it is important to note that a reduction of ϕ implies a closer free-electron behavior of the surface, resulting in an increase of the static surface dielectric constant. If $E_{i_{\mathrm{eff}}}$ varied it would lead to a reduction of $E_{k,\max}$, in contrast with the observation.

Coming to the discussion of the *effective* SDOS, the main feature maximum in region II, after a shift of 0.2–0.3 eV towards lower binding energy passing from 300 K to 500 K, remains nearly unchanged at the various temperatures investigated. A shoulder shows up in region I in the 670-K curve and persists, becoming more evident, in higher-temperature curves. The minimum of the *effective* SDOS, initially centered at 4.8 ± 0.2 eV at 300 K (region IV), widens in the direction of lower binding energy. Further, a sizeable reduction of the maximum intensity in region II (see the inset of Fig. 6) with respect to the higher-binding-energy shoulder in region III (feature *B* in Fig. 5) can be observed when passing from room temperature to 500 K.

It is worth noting that the main changes to the *effective* SDOS already take place in the 300–670 K temperature range. This effect has to be related to the first stages of surface modification around the first structure transition temperature T_1. As shown by STM,[3] disordered regions due to the motion of the adatoms are formed near domain boundaries, growing in size with increasing temperatures. This effect causes an increase of surface conductivity. Since MDS is extremely sensitive to small variations on the surface, if surface-modified regions even of small dimensions are formed, they are expected to affect MD spectra. This effect appears to be more evident in MDS than in photoemission. Different experiments have shown that some degree of metallicity, monotonically increasing, is present between 600 and 1050 K.[14,15] Nevertheless, this effect appears to be more pronounced in the present case. We believe that this is due to the enhanced surface sensitivity of MDS.

Regarding region II in the 670–1100 K temperature range, the adatom feature does not change appreciably either in energy position or in intensity. On the other hand, the increase of the well-pronounced shoulder in region I is related to the progressive depletion of states observed at about 0.8 eV and it is responsible for the observed onset shift previously discussed. The emergence of the shoulder in region I has to be related to the growth of temperature-induced states in the band gap. The data presented indicate that these states, metallic in character, are due to temperature-induced modifications of the dangling-bond states associated with the restatoms, with a less important modification of the adatom states.

C. Comparison with literature models at high temperature

To date two main mechanisms have been proposed to explain the behavior of the Ge(111) surface at temperatures around T_2 (1050 K). Molecular-dynamics simulations lead to an incomplete melting of the surface bilayer accompanied by the formation of electronic states at E_F and by a liquidlike disordering of the surface.[13] Photoemission experiments[15,16] were interpreted as giving support to this picture.

A different picture comes from high-resolution He scattering.[18] Scattering data were explained on the basis of an order-to-order transition at high temperature within a 1×1 symmetry interpreted in terms of a flattening of the surface layer through an increase of the sp^2 character of the surface back bonds and a delocalization of the adatoms.

The *effective* SDOS at high temperature (Fig. 6) has been compared with the molecular-dynamics results of incomplete molten Ge (Ref. 13) and liquid Ge.[31] Liquid and incomplete molten DOS present close similarities that are in qualitative agreement with the upward shift of the minimum at $\sim$ 4.8 eV in region IV and in the presence of states at E_F. To go further on a quantitative basis, a model calculation of the *effective* SDOS would be needed.

However, the feature assignment at room and intermediate temperatures, made on the basis of the electronic properties and the nature of the metastable deexcitation, allows us to obtain valuable information. In particular, we observed the persistence of the feature at $\sim$ 1.3 eV, associated with the adatoms, which is almost unaffected in intensity and in energy when passing from intermediate to high temperatures. We believe that this is an indication in favor of the preservation of a good degree of order. In fact evidence for long-range order at high temperature was reported by Meli *et al.*[18] using He scattering.

Moreover, the upward shift already observed at intermediate temperatures (500–670 K) of the adatom associated feature indicates some variation of the bonding condition at the adatom site that can be related to the parallel restatom contribution shift responsible of the surface metallic behavior. The upward energy shift of the adatom feature, because of its dangling-bond nature, indicates some degree of loosening of the adatom-surface interaction. Taking into account the geometrical and electronic properties of the Ge(111) surface, metallicity can be explained in terms of a tendency of the first and restatom layer to assume a planar, graphitic geometry, as proposed in Ref. 18. In this way in fact, a half-filled p_z orbital is formed producing free-electron behavior at the surface.

The present data and the state of the current understanding of the Ge(111) surface at high temperature do not allow us to be conclusive regarding the explanation of the upward shift of the features in regions III and IV. However it seems reasonable to relate the observed shift with a progressive transition towards a surface with metallic character.

A deeper and more conclusive analysis calls for theoretical calculations of the electronic structure of the flattened surface together with model calculations of the *effective*

SDOS obtained by MDS, in order to exploit further the sensitivity of the technique to the shape and the direction of the electronic orbitals.

V. CONCLUSIONS

The evolution of the surface electronic properties of the Ge(111) surface is followed from room temperature to 1100 K. The study is carried out by MDS supported by UPS.

Clear evidence of a progressive surface metallization with temperature is obtained. Metallization is accompanied by an overall shift towards lower binding energies of the features of the *effective* SDOS obtained from the experimental spectra through a deconvolution operation. One feature of the *effective* SDOS, at low binding energy ($\sim$0.8 eV at room temperature), is associated with the restatoms and is responsible of the progressive metallization of the surface while another feature, at $\sim$1.5 eV at room temperature, is ascribed to the adatoms and persists up to the higher temperatures investigated. Thanks to the surface sensitivity of the technique, a sizeable metallization is already observed in measurements at 670 K. Also, below this temperature MDS allows us to observe, with greater sensitivity than other techniques, the first stages of surface modifications leading to the $c(2\times8)\rightarrow(1\times1)$ structure transition.

Because of the different excitation mechanism, UPS shows different spectral weights of the surface-states-related features. The restatom contribution is hardly visible while bulk structures are more pronounced. The evolution of changes in UPS is monotonic, at variance with the observation reported in Refs. 15 and 16.

Differently from other studies,[14–16] for temperatures higher than 1050 K, the metallic character does not show a steplike increase. The persistence of the adatom feature, most clearly visible in MDS, indicates the preservation of an ordered surface of the type hypothesized to explain atom scattering experiments.[18] We stress that a structural change towards surface disordering would induce a drastic variation in the adatom related structure, not observed in our data.

These considerations support the so called order-order transition at high temperature[18] in contrast to an incomplete surface melting transition.[13]

ACKNOWLEDGMENTS

We are grateful to A. Santoni for supplying us with the Ge(111) samples. L. Tagliavini is acknowledged for his contribution to the experiment. E. Tosatti is acknowledged for helpful discussion. S. Ossicini and A. Patchett are acknowledged for critical reading of the paper.

*Author to whom correspondence should be addressed. FAX: +39 59 367488. Electronic address: pasquali@imoax1.unimo.it

[1] E. Tosatti, in *The Structure of Surfaces II*, edited by J. F. van der Veen and M. A. Van Hove (Springer-Verlag, Berlin, 1988), p. 535.
[2] R. J. Panheuf and M. B. Webb, Surf. Sci. **164**, 167 (1985).
[3] R. M. Feenstra, A. J. Slavin, G. A. Held, and M. A. Lutz, Phys. Rev. Lett. **66**, 3257 (1991).
[4] Zeng Gai, Hongbin Yu, and W. S. Yang, Phys. Rev. B **53**, 13 547 (1996).
[5] J. Aarts, A. J. Hoeven, and P. K. Larsen, Phys. Rev. B **38**, 3925 (1988).
[6] K. Hricovini, G. Le Lay, M. Abraham, and J. E. Bonnet, Phys. Rev. B **41**, 1258 (1990).
[7] N. Takeuchi, A. Selloni, and E. Tosatti, Phys. Rev. B **49**, 10 757 (1994).
[8] E. G. McRae and R. A. Malic, Phys. Rev. Lett. **58**, 1437 (1987); Phys. Rev. B **38**, 13 163 (1988).
[9] S. Modesti and A. Santoni, Solid State Commun. **72**, 315 (1989).
[10] M. Abraham, G. Le Lay, and J. Hila, Phys. Rev. B **41**, 9828 (1990).
[11] A. W. Denier van der Gon, J. M. Gay, J. W. M. Frenken, and J. F. van der Veen, Surf. Sci. **241**, 335 (1991).
[12] T. T. Tran, S. Thevuthasan, Y. J. Kim, D. J. Friedman, A. P. Kaduwela, G. S. Herman, and C. S. Fadley, Surf. Sci. **281**, 270 (1993).
[13] N. Takeuchi, A. Selloni, and E. Tosatti, Phys. Rev. Lett. **72**, 2227 (1994).
[14] S. Modesti, V. R. Dhanak, M. Sancrotti, A. Santoni, B. N. J. Persson, and E. Tosatti, Phys. Rev. Lett. **73**, 1951 (1994).
[15] A. Santoni, V. R. Dhanak, A. Goldoni, M. Sancrotti, and S. Modesti, Europhys. Lett. **34**, 275 (1996).
[16] A. Goldoni, A. Santoni, M. Sancrotti, V. R. Dhanak, and S. Modesti, Surf. Sci. (to be published).
[17] A. Mak, K. W. Evans-Lutterodt, K. Blum, D. Y. Noh, J. D. Brock, G. A. Held, and R. J. Birgeneau, Phys. Rev. Lett. **66**, 2002 (1991).
[18] C. A. Meli, E. F. Greene, G. Lange, and J. P. Toennies, Phys. Rev. Lett. **74**, 2054 (1995).
[19] See, for example, H. D. Hagstrum, in *Chemistry and Physics of Solid Surfaces VII*, edited by R. Vanselow and R. Rowe (Springer-Verlag, Berlin, 1988), p. 341; W. Sesselmann, B. Woratschek, J. Küppers, G. Ertl, and H. Haberland, Phys. Rev. B **35**, 1547 (1987).
[20] L. Pasquali, S. Nannarone, M. Canepa, and L. Mattera, Phys. Rev. B **52**, 17 355 (1995).
[21] M. Biagini, S. Ossicini, L. Pasquali, and S. Nannarone (unpublished).
[22] G. Paolicelli, G. Panaccione, R. Cosso, S. Kaciulis, S. Nannarone, I. Abbati, M. Canepa, S. Terreni, and L. Mattera, Vuoto **23**, 106 (1994).
[23] R. J. Bringans, and H. Höchst, Phys. Rev. B **25**, 1081 (1982).
[24] R. J. Bringans, R. I. G. Uhrberg, and R. Z. Bachrach, Phys. Rev. B **34**, 2373 (1986).
[25] J. M. Nicholls, G. V. Hansson, R. I. G. Uhrberg, and S. A. Flodström, Phys. Rev. B **33**, 5555 (1986).
[26] J. Aarts, A. J. Hoeven, and P. K. Larsen, Phys. Rev. B **37**, 8190 (1988).
[27] S. M. Sze, in *Physics of Semiconductor Devices*, 2nd ed. (Wiley, New York, 1982).
[28] T. Sakurai and H. D. Hagstrum, Phys. Rev. B **20**, 2423 (1979).
[29] H. D. Hagstrum and G. E. Becker, Phys. Rev. B **4**, 4187 (1971).
[30] N. Takeuchi, A. Selloni, and E. Tosatti, Phys. Rev. Lett. **69**, 648 (1992).
[31] W. Jank and J. Hafner, Europhys. Lett. **7**, 623 (1988).